

Sign Problem in Quantum Monte Carlo Simulation

Gaopei Pan^{a,b}, Zi Yang Meng^c

^aBeijing National Laboratory for Condensed Matter Physics and Institute of Physics, Chinese Academy of Sciences, Beijing 100190, China

^bSchool of Physical Sciences, University of Chinese Academy of Sciences, Beijing 100190, China

^cDepartment of Physics and HKU-UCAS Joint Institute of Theoretical and Computational Physics, The University of Hong Kong, Pokfulam Road, Hong Kong SAR, China

Abstract

Sign problem in quantum Monte Carlo (QMC) simulation appears to be an extremely hard yet interesting problem. In this article, we present a pedagogical overview on the origin of the sign problem in various quantum Monte Carlo simulation techniques, ranging from the world-line and stochastic series expansion Monte Carlo for boson and spin systems to the determinant and momentum-space quantum Monte Carlo for interacting fermions. We point out the basis dependency of the sign problem and summarize the progresses to cure, ease and even make use of the sign problem over the years, such as symmetry analysis of the underlying Hamiltonian, basis optimization in writing down the partition functions and many others. Moreover, we state that although traditional lore saying that in case of sign problem, the average sign in QMC simulation approaches zero exponentially fast with the space-time volume of the configurational space, there are recent breakthroughs showing this is not always the case and based on the properties of the partition function for finite size systems, one could distinguish when the average sign has the usual exponential scaling and when it is bestowed with an algebraic scaling at the low temperature limit. Fermionic QMC simulations with such algebraic sign problems have been successfully carried out for extended Hubbard-type and quantum Moiré lattice models.

Keywords:

Sign Problem, Quantum Monte Carlo, Strongly correlated electrons

1. Introduction

Quantum Monte Carlo (QMC) method is an extremely powerful and unbiased method for studying strongly correlated systems, especially in condensed matter, high energy and quantum material research [1, 2, 3, 4, 5], where the quantum many-body lattice models are in general analytically intractable. In QMC simulation, the partition function of the interacting problem is cast into a sum (or integral) over configurations in a chosen basis, and the important sampling scheme could in principle cover the exponentially large configurational space in polynomial time.

However, such practice is oftentimes hindered by the infamous "Sign Problem" [6]. Sign problem means the weights of configurations in the QMC simulation become negative or even complex, and therefore the configurational weights in the Monte Carlo process cannot be further interpreted as classical probabilities, and the minus or even complex sign will rendered the QMC simulation with exponential complexity for obtaining the data with the same quality compared with the simulations without sign problem. It has been proved that if we could find a method to solve nondeterministic polynomial (NP) hard problem efficiently, the method can be used to solve the QMC simulations with the sign problem [7]. It's important to note that this doesn't mean the sign problem is considered to be NP-hard [8], nor is it inconsistent with performing polynomial-time QMC simulation of specific cases that have negative or complex sign.

The origin of the sign problem has no universal explanation, but it is believed to come from the quantum mechanic properties of the constituent particles in the many-body systems, given them fermions, bosons or spins. Frustrated spin systems often have a sign problem because the off-diagonal operators in the Hamiltonian usually bring a negative amplitude [9, 10] and the number of off-diagonal operators can be odd for a particular configuration. While in fermionic systems, negative weights usually arise from the Pauli exclusion principle [7] or different Hubbard-Stratonovich decoupling [11] scheme (which means decoupling the quartic fermion interaction term into certain quadratic basis). At

the same time, there are also proposals that the negative sign of a configuration is a topological invariant, which is an imaginary time counterpart of the Aharonov-Anandan phase and can be reduced to a Berry phase in the adiabatic limit [12]. And the sign problem has even been linked to quantum phase transitions [13, 14]. Moreover, it was shown recently that some interacting models may have intrinsic sign problem, which cannot be cured [15, 16, 17, 18]. In general, an unified description of the sign problem is still missing. These different situation where the sign problem occur in QMC simulations will be discussed in a case based manner in Secs. 2 and 3 of this article.

Fortunately, there are many cases of quantum lattice models where there are no or weak (polynomial instead of exponential scaling) sign problems and Monte Carlo calculations can be carried out with polynomial complexity. In frustrated magnet lattice models, there is no sign problem for some bilayer models [19, 20, 21, 22, 23] within certain parameters. Inspired by the absence of sign problems in the above models, one can choose those models as sign-problem-free reference system and extend the simulation basis from spin to singlet-triplet or even plaquette bases, and it has been shown the QMC simulations can be carried out to the parameter space for few important 2D frustrated lattice models (such as the Shastry-Sutherland antiferromagnetic spin model) where there were sign problem in the original spin basis [24, 25]. Interacting fermion models (mainly Hubbard-type) at certain basis with certain symmetries, such as anti-unitary symmetry, have been proved to be sign problem free [26, 27, 28, 29]. Flat band quantum Morie lattice models with $C_2T + C_2P$ symmetries can also ensure that there are no sign problems [30, 31, 32, 33]. There also exist cases where one can use Majorana representation to avoid the sign problem, to split the fermionic operator into Majorana fermions and reuse the anti-unitary symmetry [34, 35, 36, 37, 38]. In addition, basis transformation [39, 40, 41, 42, 43, 44, 45, 46, 47, 48], Lefschetz thimbles [49, 50], meron cluster [51], Fermi bags [52], split-orthogonal group [38], Majorana positivity [37], semigroup approach [53] and pseudo-unitary group [54], automatic differentiation [55], machine learning techniques [56, 57] and adiabatic method [58], or through some systematic expansion[59] can also solve or ease some sign problems. These cases will be discussed in Secs. 4 and 5 of this article.

If there is sign problem in the QMC simulation, the usual simulation approach is to reweight: one can take the magnitude of the original weight (or magnitude of the real part) as the new weight, and add the sign into the sampling process of physical observables and divide the average sign $\langle s \rangle$. This approach does not solve the sign problem, but only cast it into a different form. The average sign over the Monte Carlo sampling will appear in the denominator, so the average sign will affect how long it will take to obtain meaningful expectation values with controlled errorbars in the simulation. Usually $\langle s \rangle \propto e^{-N\beta\Delta f}$ where Δf is the free energy difference of the two systems before and after the Monte Carlo update. This means sign often decay exponentially. And there are a lot of research which support viewpoint. No matter what lattice (hypercubic, ladder, depleted square, Lieb, honeycomb, kagome, and triangular lattices) or parameter (temperature, interaction strength, and density), the sign usually decay exponentially. There is a good summary [60] of the sign datas for different geometry and parameters.

But Recent developments have changed this viewpoint, there are cases in Hubbard model at certain filling the average sign is not exponential decay [61, 62] and we have found that it is possible to prove the average sign of quantum many-body lattice models acquire algebraic sign structure [32, 33], if their finite size partition functions satisfy the *Sign bound theory*. The details on the theory and its application on the systems with extended or long-range interaction such as the extended Hubbard [32, 63] and quantum Moiré lattice models [64, 65, 66, 30, 67, 33, 68], are given in Sec. 5.3 of this article.

2. Configurational weight in classical Monte Carlo simulation

Before presenting the details of the sign problem, we first discuss classical Monte Carlo simulation briefly such that the origin of the sign problem manifests naturally.

In classical Monte Carlo, the partition function at temperature T is written as follows:

$$Z = \text{Tr}[e^{-\beta H}] = \sum_{C \in \Omega} e^{-\beta E(C)} = \sum_{C \in \Omega} W(C) \quad (1)$$

where $\beta = \frac{1}{k_B T}$, k_B is the Boltzmann constant, and C stands for the configurations in the configurational space Ω , which is exponentially large in system size, such as 2^{L^d} and 4^{L^d} for d dimensional spin or fermion systems with linear dimension L . Once the partition function is written as a sum of Boltzmann weights $e^{-\beta E(C)}$, it's clear that in the classical

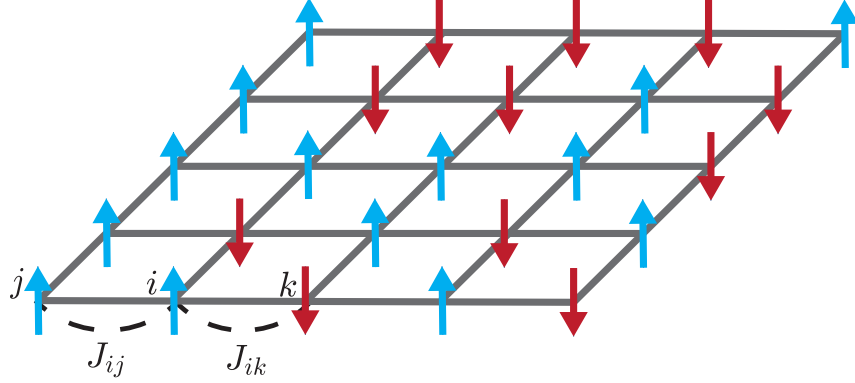


Figure 1: Classical Ising configuration of the example $E(C) = \sum_{i,j} E_{i,j}$ and $E_{i,j} = J_{i,j}$ and $E_{i,k} = -J_{i,k}$.

Monte Carlo the $W(C)$ corresponding to different configurations are always positive and real numbers. So one can easily carry Monte Carlo updates in Markov chain by calculating the ratio of weights of different configurations.

For example, as shown in Fig. 1, the Hamiltonian of the classical 2d Ising model is: $H = \sum_{i,j} J_{i,j} s_i s_j$, where s_i denotes the state of the i -th spin which takes the value of ± 1 (up or down), $J_{i,j}$ is the interaction strength. For the configuration in Fig. 1, the corresponding weight is $e^{-\beta \sum_{i,j} E_{i,j}(C)}$.

We know the expectation values of observable O is:

$$\langle O \rangle = \frac{1}{Z} \text{Tr}[O e^{-\beta H}] = \frac{1}{Z} \sum_{C \in \Omega} O(C) W(C). \quad (2)$$

For the classical case, since $W(C)$ is a real number and $W(C) \geq 0$, one can carry out the Monte Carlo and obtain N_b configurations $\{C_i\}$ from Ω , according to the distribution $p(C_i) = W(C_i)/Z$. Here N_b is number of sampling bins, and then the average value of the samples is the expectation value of the physical quantity O :

$$\langle O \rangle \approx \bar{O} = \frac{1}{N_b} \sum_{i=1}^{N_b} O(C_i). \quad (3)$$

The statistical error corresponding to such an estimate of the mean value is [69]:

$$\Delta O = \sqrt{\frac{\text{Var}(O) 2\tau_O^{\text{int}}}{N_b}}, \quad (4)$$

where $\text{Var}(O)$ is the variance of O and the integrated autocorrelation time τ_O^{int} is a measure of the autocorrelations of the sequence $\{O(C_i)\}$

$$\tau_O^{\text{int}} = \frac{1}{2} + \sum_{t=1}^{\infty} A_O(t), \quad (5)$$

and the autocorrelation function $A_O(t)$ for a quantity O is defined as:

$$A_O(t) = \frac{\langle O(C_{i+t}) O(C_i) \rangle - \langle O \rangle^2}{\langle O^2 \rangle - \langle O \rangle^2}. \quad (6)$$

In principle, since in classical Monte Carlo weights are always real and positive and the statistical errors are inversely proportional to the number of bins $\Delta O \propto \frac{1}{\sqrt{N_b}}$. One can carry out Monte Carlo sampling in polynomial time to achieve controlled expectation values (critical slowing down is not taken into account).

3. Configurational weight in quantum Monte Carlo simulation

However when we consider quantum Monte Carlo (QMC) simulation, the weight may become a negative or even a complex number and cause the sign problem in the sampling. In QMC, quantum many-body problems in d dimension are usually mapped onto a classical system in $d + z$ dimension, where z is the dynamic exponent of the problem and usually taken to be 1 in practical simulations [70]. Depending on the quantum lattice models, there are many different QMC algorithms, such as world-line Monte Carlo [70, 71, 72, 73], stochastic series expansion (SSE) [74, 75], determinant quantum Monte Carlo (DQMC) [11, 76], momentum space quantum Monte Carlo [30, 67, 77] and so on. The form of the weights in these methods and the origin of sign problem are not the same and we will discuss them one by one.

3.1. World-Line Monte Carlo

The usual world-line approach [70, 71, 72, 78, 73, 79] starts with discretizing the inverse temperature β , and employing the Suzuki-Trotter approximation [80, 81, 82, 83] to decompose the exponential of the Hamiltonian. A common world-line expansion of the partition function is:

$$\begin{aligned} Z &= \text{Tr}[e^{-\beta\hat{H}}] = \text{Tr}[e^{-M\Delta\tau\hat{H}}] = \text{Tr}\left[\left(e^{-\Delta\tau\hat{H}_1}e^{-\Delta\tau\hat{H}_2}\right)^M\right] + O(\Delta\tau^2) \\ &= \sum_{i_1, \dots, i_{2M}} \langle i_1 | e^{-\Delta\tau\hat{H}_1} | i_{2M} \rangle \langle i_{2M} | e^{-\Delta\tau\hat{H}_2} | i_{2M-1} \rangle \dots \\ &\quad \langle i_3 | e^{-\Delta\tau\hat{H}_1} | i_2 \rangle \langle i_2 | e^{-\Delta\tau\hat{H}_2} | i_1 \rangle \end{aligned} \quad (7)$$

where $|i_l\rangle\langle i_l|$, $l \in [1, 2M]$ are the complete basis of the quantum many-body problem and they are inserted between the imaginary time evolution operators. Separating $\hat{H} = \sum_i \hat{H}_i$ in such a way to facilitate the calculation of matrix elements make it easy to consider the sign problem. We can see that the matrix elements $\langle i | e^{-\Delta\tau\hat{H}_k} | j \rangle$ in the weights of a worldline configuration are not obviously positive or negative, therefore, we in general don't know whether the product of these matrix elements is a positive real number.

For example, for spin-1/2 XXZ model in a chain, with Hamiltonian:

$$\hat{H} = J_x \sum_i (\hat{S}_i^x \hat{S}_{i+1}^x + \hat{S}_i^y \hat{S}_{i+1}^y) + J_z \sum_i \hat{S}_i^z \hat{S}_{i+1}^z. \quad (8)$$

We can split it in such a way:

$$\hat{H} = \underbrace{\sum_n \hat{H}^{(2n+1)}}_{\hat{H}_1} + \underbrace{\sum_n \hat{H}^{(2n+2)}}_{\hat{H}_2} \quad (9)$$

where $\hat{H}^{(i)} = J_x (\hat{S}_i^x \hat{S}_{i+1}^x + \hat{S}_i^y \hat{S}_{i+1}^y) + J_z \hat{S}_i^z \hat{S}_{i+1}^z$. By introducing spin flip operators $\hat{S}_j^\pm = \hat{S}_j^x \pm i\hat{S}_j^y$, we can write configurations in the spin representation. An example of QMC configuration and values of matrix elements can be seen in Fig 2. In this case, although the corresponding weight of spin flip is negative, the periodic boundary condition guarantees that the number of spin flips must be even, so the total weight must be positive. But for other cases, there may not be similar conditions to ensure that the weight is positive.

For continuous-time world-lines, the expansion may vary, but the form of the weights is broadly similar:

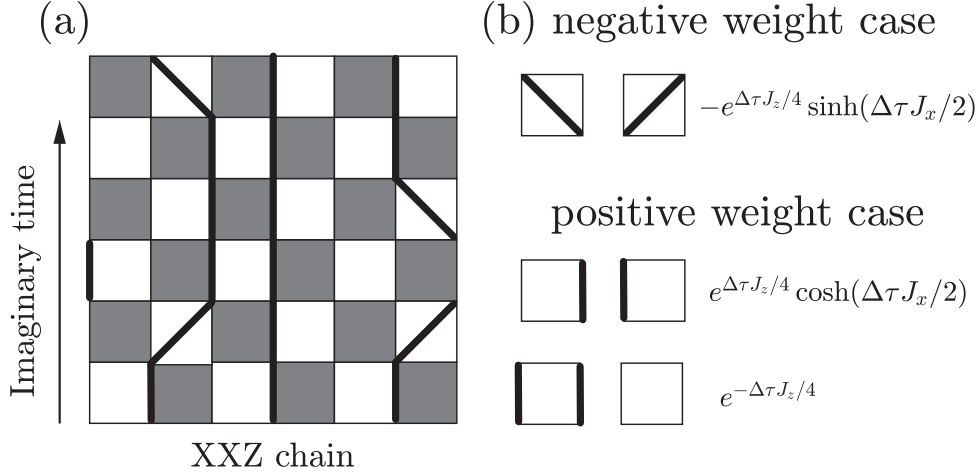


Figure 2: World line configuration for the XXZ model. (a). The bold lines correspond to the imaginary time evolution of spin up states, and the unpassed points correspond to states with spin down. (b). Corresponding weights of matrix elements in different cases. We see that the negative weight case corresponds to the spin flip operation.

If $\hat{H} = \hat{H}_0 + \hat{V}$, and \hat{V} is a perturbation [84]. We define $e^{-\tau\hat{H}_0}\hat{U}(\tau) = e^{-\tau(\hat{H}_0+\hat{V})}$ and $\hat{V}(\tau) = e^{\tau\hat{H}_0}\hat{V}e^{-\tau\hat{H}_0}$. Then

$$\begin{aligned}
Z &= \text{Tr} \left[e^{-\beta\hat{H}_0} \hat{U}(\beta) \right] \\
&= \text{Tr} \left[e^{-\beta\hat{H}_0} \left(1 - \int_0^\beta d\tau_1 \hat{V}(\tau_1) + \int_0^\beta d\tau_2 \int_0^{\tau_2} d\tau_1 \hat{V}(\tau_2) \hat{V}(\tau_1) - \dots \right) \right] \\
&= \text{Tr} \left[\sum_{n=0}^{\infty} (-1)^n \int_0^\beta d\tau_n \int_0^{\tau_n} d\tau_{n-1} \dots \int_0^{\tau_2} d\tau_1 e^{-(\beta-\tau_n)\hat{H}_0} \hat{V} e^{-(\tau_n-\tau_{n-1})\hat{H}_0} \times \hat{V} \dots \hat{V} e^{-\tau_1\hat{H}_0} \right] \\
&= \sum_{n=0}^{\infty} (-1)^n \sum_{\phi_n, \dots, \phi_1} \int_0^{\tau_2} d\tau_n \int_0^{\tau_n} d\tau_{n-1} \dots \int_0^{\tau_2} d\tau_1 \langle \phi_1 | e^{-(\beta-\tau_n)\hat{H}_0} | \phi_1 \rangle \langle \phi_1 | \hat{V} | \phi_n \rangle \\
&\quad \times \langle \phi_n | e^{-(\tau_n-\tau_{n-1})\hat{H}_0} | \phi_n \rangle \langle \phi_n | \hat{V} | \phi_{n-1} \rangle \dots \langle \phi_2 | \hat{V} | \phi_1 \rangle \langle \phi_1 | e^{-\tau_1\hat{H}_0} | \phi_1 \rangle
\end{aligned} \tag{10}$$

where $\hat{U}(\tau) = 1 - \int_0^\tau d\tau' \hat{V}(\tau') \hat{U}(\tau')$.

3.2. Stochastic Series Expansion

Stochastic series expansion (SSE) method [74, 75] Taylor expands the partition function, and it can be shown that the expansion of finite size systems can be safely truncated,

$$\begin{aligned}
Z &= \text{Tr}[\exp^{-\beta\hat{H}}] = \sum_{n=0}^{\infty} \frac{(-\beta)^n}{n!} \text{Tr}[\hat{H}^n] \\
&= \sum_{n=0}^{\infty} \sum_{i_1, \dots, i_n} \frac{(-\beta)^n}{n!} \langle i_1 | \hat{H} | i_2 \rangle \langle i_2 | \hat{H} | i_3 \rangle \dots \langle i_n | \hat{H} | i_1 \rangle \\
&\equiv \sum_{n=0}^{\infty} \sum_{i_1, \dots, i_n} p(i_1, \dots, i_n) \equiv \sum_{C \in \Omega} W(C)
\end{aligned} \tag{11}$$

which is similar to the case of the world-line, the final sign of the weight is also determined by the number of negative matrix elements multiplied, i.e., usually by the number of off-diagonal elements (on the spin \hat{S}_i^z basis, the spin flip

term $\hat{S}_j^+ \hat{S}_{j+1}^- + \hat{S}_j^- \hat{S}_{j+1}^+$ is off-diagonal). For bipartite lattices such as square or honeycomb with periodic boundary condition in space-time, it can be shown that the number of the off-diagonal operator is always even such that their product in the configurational weight will be positive, however, for non-bipartite lattices, such as triangle and kagome, the number of the off-diagonal operators can be odd and the SSE simulation will have sign problem. We note that there are recent developments in frustrated magnet lattice models, some bilayer models [19, 20, 21, 22, 23] within certain parameters with cluster basis are sign-problem-free. Inspired by these works and considering the model that has the same ground state as the above model, one can extend the simulation basis from spin to singlet-triplet or even plaquette bases, and it has been shown the SSE-QMC simulations for few important 2D frustrated lattice model, such as the Shastry-Sutherland antiferromagnetic spin model, can be carried out to the parameter space where there were sign problem in the original spin basis [24, 25].

3.3. DQMC

For interacting fermion models, one use different ways to write down the partition functions. In determinant quantum Monte Carlo (DQMC) [11, 76], auxiliary fields are introduced to decouple interactions through Hubbard-Stratonovich transformation. Taking Hubbard model as an example, Suzuki-Trotter decomposition is still necessary:

$$Z = \text{Tr} \left[e^{-\Delta\tau \hat{H}_I} e^{-\Delta\tau \hat{H}_0} e^{-\Delta\tau \hat{H}_I} e^{-\Delta\tau \hat{H}_0} \dots e^{-\Delta\tau \hat{H}_I} e^{-\Delta\tau \hat{H}_0} \right] \quad (12)$$

where $\hat{H}_0 = -t \sum_{\langle i,j \rangle} (\hat{c}_i^\dagger \hat{c}_j + h.c.)$ and $\hat{H}_I = U \sum_i (\hat{n}_{i\uparrow} - \frac{1}{2})(\hat{n}_{i\downarrow} - \frac{1}{2})$. $\langle i, j \rangle$ means nearest-neighbour hopping. Then Hubbard-Stratonovich transformation gives:

$$\begin{aligned} e^{-\Delta\tau \hat{H}_I} &= \prod_i e^{-\Delta\tau U (\hat{n}_{i\uparrow} - \frac{1}{2})(\hat{n}_{i\downarrow} - \frac{1}{2})} \\ &= \prod_i \gamma \sum_{s_{i,l}=\pm 1} e^{\alpha s_{i,l} (\hat{n}_{i\uparrow} - \hat{n}_{i\downarrow})} \\ &= \gamma^N \sum_{s_{i,l}=\pm 1} \left(\prod_i e^{\alpha s_{i,l} \hat{n}_{i\uparrow}} \prod_i e^{-\alpha s_{i,l} \hat{n}_{i\downarrow}} \right) \end{aligned} \quad (13)$$

where $\gamma = \frac{1}{2} e^{-\Delta\tau U/4}$, $\cosh(\alpha) = e^{\Delta\tau U/2}$.

Since we have $\text{Tr} \left[e^{-\sum_{i,j} \hat{c}_i^\dagger A_{i,j} \hat{c}_j} e^{-\sum_{i,j} \hat{c}_i^\dagger B_{i,j} \hat{c}_j} \right] = \text{Det} (1 + e^{-\mathbf{A}} e^{-\mathbf{B}})$, then partition function is:

$$\begin{aligned} Z &= \sum_{s_{i,l}=\pm 1} \gamma^{NL_\tau} \text{Tr}_F \left\{ \prod_{l=1}^{L_\tau} \left[\left(\prod_i e^{\alpha s_{i,l} \hat{n}_{i\uparrow}} \right) \left(e^{-\Delta\tau c_\uparrow^\dagger T c_\uparrow} \right) \left(\prod_i e^{-\alpha s_{i,l} \hat{n}_{i\downarrow}} \right) \left(e^{-\Delta\tau c_\downarrow^\dagger T c_\downarrow} \right) \right] \right\} \\ &= \gamma^{NL_\tau} \sum_{\{s_{i,l}\}} \prod_{\sigma=\uparrow\downarrow} \text{Det} [\mathbf{I} + \mathbf{B}^\sigma (L_\tau \Delta\tau, (L_\tau - 1) \Delta\tau) \dots \mathbf{B}^\sigma (\Delta\tau, 0)] \end{aligned} \quad (14)$$

where

$$\begin{aligned} \mathbf{B}^\uparrow (l_2 \Delta\tau, l_1 \Delta\tau) &= \prod_{l=l_1+1}^{l_2} e^{\alpha \text{Diag}(\vec{s}_l)} e^{-\Delta\tau T} \\ \mathbf{B}^\downarrow (l_2 \Delta\tau, l_1 \Delta\tau) &= \prod_{l=l_1+1}^{l_2} e^{-\alpha \text{Diag}(\vec{s}_l)} e^{-\Delta\tau T} \end{aligned} \quad (15)$$

and $\text{Diag}(\vec{s}_l)$ is a diagonal matrix with diagonal elements $s_{i,l}$. For the space-time configuration $\{s_{i,l}\}$, the calculation of weight is converted to the calculation of the determinant of matrices. Without a prior knowledge such as symmetry analysis or energy spectrum [33], the determinant of a matrix doesn't have to be a positive real number. It is worth noting that the Hubbard-Stratonovich transformation which introduce auxiliary field is also one of the causes of the sign problem. For example, using the world-line method, the one-dimensional Hubbard model has no sign problem[3, 73], but for DQMC, usually there is a sign problem[60].

A Markov chain for the DQMC simulation for the 2d Hubbard model, with $L \times L \times \beta$ and the auxiliary fields for three consecutive configurations are given in Fig. 3.

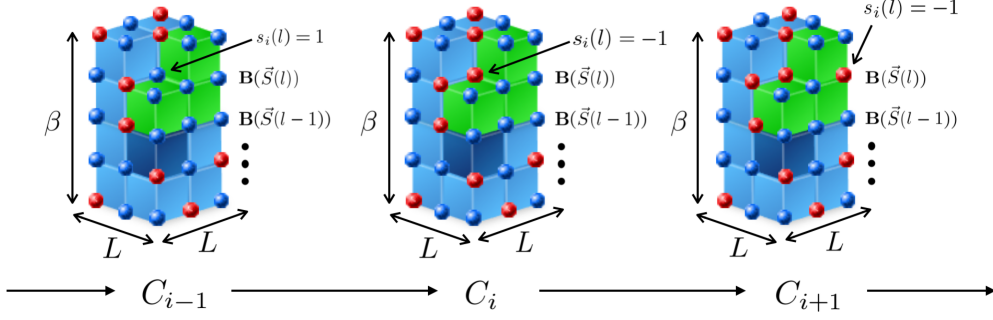


Figure 3: The space-time auxiliary field $\{s_{i,l}\}$ introduced by Hubbard-Stratonovich transformation lives on the lattice of $d+1$ dimension (here $d=2$ with linear system size L), and we perform the calculation of Markov chain Monte Carlo by flipping the auxiliary field on the space-time lattice with the corresponding probability. Here the notation $\mathbf{B}(\vec{S}(l))$ corresponds to the matrix containing the auxiliary field of imaginary time layer l , shown in Eq. (15).

4. What is the Sign Problem?

With the above preparation, we now discuss the real content of the sign problem. As the name implies, the simplest and most straightforward definition of the sign problem is that, the weights (probabilities) in the Monte Carlo simulation $p(C_i) = W(C_i)/Z$ is negative or becomes a complex number.

For the real time evolution of a quantum mechanic state, this is obviously going to happen, because the time evolution operator is e^{-itH} and the corresponding configurational weight $W(C) \sim \exp(iS(C))$, here $S(C)$ is the action function of configuration C , which is time integral of Lagrangian L : $S = \int dt L(x, \dot{x})$. It's not surprising that now the weight might be a complex number. While if we consider the ensemble average at the thermal equilibrium state for classical statistical problems such as the Ising model in Sec. 2, configurational weight $W(C) \sim \exp(-\beta H(C))$, is real and positive.

When we discuss algorithms that do not suffer from the sign problem [7], it usually means that the algorithm needs polynomial complexity to evaluate the thermal average $\langle O \rangle$, i.e. with the system size $N = L^d$ and inverse temperature $\beta = 1/k_B T$, the computational time required to make the relative error $\Delta O / \langle O \rangle$ less than ϵ is called $t(\epsilon, N, \beta)$. If $t(\epsilon, N, \beta)$ grows polynomially with N and β , i.e. there exist integers n and m and a constant $\kappa < \infty$ such that

$$t(\epsilon, N, \beta) < \kappa \epsilon^{-2} N^n \beta^m. \quad (16)$$

Such complexity is tractable with realistic Monte Carlo simulation in both human and machine time.

One thing needs to clarify is that sign problem doesn't mean one can not carry out Monte Carlo simulation on finite size system. If there is sign problem, the usual expedient [6] is to introduce a reference system which is sign-problem-free, by reweighting:

$$\langle O \rangle = \frac{\sum_C O(C_i) W(C_i)}{\sum_C W(C_i)} = \frac{\sum_C O(C_i) s(C_i) |W(C_i)|}{\sum_C s(C_i) |W(C_i)|} \frac{\sum_C |W(C_i)|}{\sum_C |W(C_i)|} \equiv \frac{\langle O s \rangle'}{\langle s \rangle'} \quad (17)$$

where $s(C_i) = \frac{W(C_i)}{|W(C_i)|}$ and $\langle O \rangle' = \frac{\sum_C O(C_i) |W(C_i)|}{\sum_C |W(C_i)|}$. The average of sign: $\langle s \rangle = Z/Z'$, which is just the ratio of the partition function of the system $Z = \sum_C W(C_i)$ with weights $W(C_i)$ and the reference system used for sampling with another partition function $Z' = \sum_C |W(C_i)|$.

As the partition function is usually an exponential form of the free energy, then $\langle s \rangle = Z/Z' = \exp(-\beta N \Delta f)$, where Δf is the free energy densities differences of Z and Z' . When there is a sign problem, the term $\langle s \rangle'$ in the denominator needs to be taken into account when calculating the mean value of quantity, so the relative error $\Delta s / \langle s \rangle$ of the sign are very important, and it usually increases exponentially with inverse temperature β and system size N :

$$\frac{\Delta s}{\langle s \rangle} = \frac{\sqrt{(\langle s^2 \rangle - \langle s \rangle^2) / N_b}}{\langle s \rangle} = \frac{\sqrt{1 - \langle s \rangle^2}}{\sqrt{N_b} \langle s \rangle} \sim \frac{e^{\beta N \Delta f}}{\sqrt{N_b}} + O(\langle s \rangle) \quad (18)$$

where N_b is number of bins. In most cases, Δf is a quantity that doesn't change very much in the simulation, so when there is a sign problem, the QMC simulation usually takes exponential time to have a reasonable estimation of the errorbars for physical observables.

The exponential computation time seems to imply that sign problem may be a nondeterministic polynomial (NP) problem, but is it an NP-hard problem? Here NP problem is the set of decision problems solvable in polynomial time by a nondeterministic Turing machine, and a NP-hard problem means every problem in NP can be reduced in polynomial time to it. At present, the answer still seems unclear, but explicit examples can deepen our understanding.

People try to construct a simulation with sign problem, and the calculation of its physical quantity can be transformed into a solution of a NP-complete problem. Here a problem is NP-complete means it is both NP and NP-hard. It is suggested that if the polynomial time solution corresponding to the sign problem is found, the polynomial time solution of the NP-complete problem can also be found, that is, the sign problem is a NP-hard problem. In Ref. [7], people consider a well-known special case of the classical Ising spin glass model. One can map it to NP-hard graph problem, such as 'finding ground energy' to another problem 'finding a cocycle of minimum weight while a two-level grid $G = (V, E)$, and a weighting function $J : E \rightarrow \{-1, 0, 1\}$ are given' [85]. Here a graph $G = (V, E)$ consists of a set of vertices V , and a set E of unordered pairs of different vertices, called edges. Then it is possible to introduce a corresponding NP-complete problem [7]: for given constant C , does the ground state have energy $E_0 \leq C$? And then one can map the classical Ising spin glass model to quantum Ising spin glass model with $\sigma_i^x \sigma_j^x$ term, which has sign problem. Mathematically, because this problem is NP-complete, there exists a polynomial time mapping to any other NP-complete problem.

However, the special spin glass example is equivalent to saying quantum spin glass problem is no easier to solve than the corresponding classical spin glass problem. The example is very special and the proof does not address QMC solutions of systems, such as Hubbard model without particle-hole symmetry and SU(2) frustrated quantum spin models, which are not directly associated with the difficulties of simulating classical frustrated glassy systems with complicated energy landscapes. So we can not conclude that all sign problems are NP-hard. But from this example, at least we know that if we find a method to solve an NP-hard problem, this scheme can be used to solve QMC simulation with sign problem.

In addition, the definition $\langle s \rangle = Z/Z'$ can give us some other information. Just write it in zero-temperature limit:

$$\langle s \rangle_R = \frac{Z}{Z^R} = \frac{g e^{-\beta E_0}}{g^R e^{-\beta E_0^R}} \quad (19)$$

where g and g^R are the ground state degeneracy of systems Z and reference system Z^R , while E_0 and E_0^R are ground energy of systems Z and Z^R . This means the expectation value $\langle s \rangle_R$ can be used to read g , E_0 for finite size systems, if we engineer the reference system with known g^R and E_0^R .

For spin system case, if the systems Z and reference system Z^R have same ground state, and the ground is in the set of QMC computational basis, one can see reduction of the sign problem at low-temperature, as shown in Refs. [24, 25]. For fermion case, we can also choose a good reference system Z^R , or choose a well-known $Z' \geq Z^R$ to get the lower bound of the sign, this will be explained in the *Sign bound theory* in Sec. 5.3.

Now we know the definition of sign problem, then what is sign problem related to? The collective efforts over the years have pointed out the sign problem have multiple origins. And we will discuss the major ones below.

4.1. Sign Problem is basis-dependent

First of all, the sign problem is basis-dependent. For example, if one can diagonalize the Hamiltonian matrix and calculate the eigenstates $\{|i\rangle\}$ then $H|i\rangle = \varepsilon_i|i\rangle$ and

$$\begin{aligned} \langle O \rangle &= \text{Tr}[O \exp(-\beta H)] / \text{Tr}[\exp(-\beta H)] \\ &= \sum_i \langle i|O|i\rangle \exp(-\beta \varepsilon_i) / \sum_i \exp(-\beta \varepsilon_i). \end{aligned} \quad (20)$$

There's obviously no sign problem here. Unfortunately, it is often difficult to obtain eigenstates of a quantum many-body system in the first place. Moreover, if one already has the methods to obtain all eigenstates of the system, there is then no need to perform Monte Carlo simulations.

In addition, for interacting fermion systems, different basis will bring different effects during decoupling. In a recent paper on automatic differentiation to mitigating the sign [55], the authors performed different decoupling at different sites $e^{-\Delta\tau U(\hat{n}_{i1}-\frac{1}{2})(\hat{n}_{i1}-\frac{1}{2})} = \frac{1}{2}e^{-U\Delta\tau/4} \sum_{s_i=\pm 1} e^{\Delta s_i \hat{c}_i^\dagger \sigma \cdot \mathbf{n}_i \hat{c}_i}$, where $\mathbf{n}_i = (\sin \theta_i \sin \phi_i, \sin \theta_i \cos \phi_i, \cos \theta_i)$. The choice of basis for decoupling at different sites can affect the severity of sign problem. While for spin systems, as discussed in Eq. (19), if the ground state is a member of the computational basis, and sign-problem-free reference system have the same ground state, reduction of the sign problem at low-temperature [24, 25] will be seen.

We note there exist many research works that mitigate the sign problem by basis transformation [39, 40, 41, 42, 43, 44, 45, 46, 47, 48]. However, it has also been pointed out that some sign problems turn out to be intrinsic [15, 16, 17, 18] and cannot be eliminated by local unitary basis transformations.

4.2. Sign Problem is related to Pauli exclusion principle

From the point of view of world-line Monte Carlo, the exchange of fermions in the world-line will bring a minus sign, which arise from the Pauli exclusion principle. A simple such process is shown in Fig. 4 and can be derived as

$$\begin{aligned} \langle \psi_1 | \hat{c}_1^\dagger \hat{c}_4 \hat{c}_3^\dagger \hat{c}_2 \hat{c}_4^\dagger \hat{c}_3 \hat{c}_2^\dagger \hat{c}_1 | \psi_1 \rangle &= \langle \psi_1 | \hat{c}_4 \hat{c}_3^\dagger \hat{c}_2 \hat{c}_4^\dagger \hat{c}_3 \hat{c}_2^\dagger \hat{n}_1 | \psi_1 \rangle \\ &= \langle \psi_1 | \hat{c}_4 \hat{c}_3^\dagger \hat{c}_4^\dagger \hat{c}_3 (1 - \hat{n}_2) \hat{n}_1 | \psi_1 \rangle \\ &= -\langle \psi_1 | (1 - \hat{n}_4) \hat{n}_3 (1 - \hat{n}_2) \hat{n}_1 | \psi_1 \rangle \\ &= -\langle \psi_1 | \psi_1 \rangle. \end{aligned} \quad (21)$$

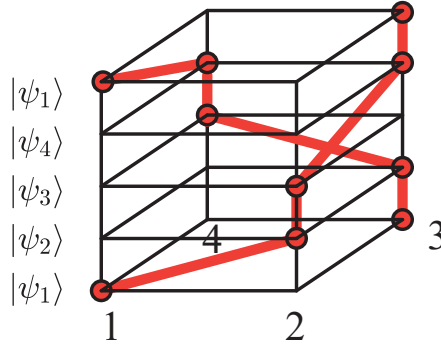


Figure 4: An example of a configuration where particle exchange leads to negative weights. The dots represent particle occupation, and blod lines are world lines.

4.3. Sign Problem is related to geometric Frustration

Similarly, frustrated spin or boson systems often have sign problem. For example, if we consider a boson (spin) system of three sites:

$$\hat{H} = (\hat{b}_1^\dagger \hat{b}_2 + \hat{b}_2^\dagger \hat{b}_3 + \hat{b}_3^\dagger \hat{b}_1) + \text{h.c.} \quad \text{or} \quad \hat{H} = (\hat{S}_1^+ \hat{S}_2^- + \hat{S}_2^+ \hat{S}_3^- + \hat{S}_3^+ \hat{S}_1^-) + \text{h.c.} \quad (22)$$

The weight is negative for the following configuration (where $|i\rangle$ means i -th site occupied state):

$$\langle 1 | e^{-d\beta \hat{H}} | 2 \rangle \langle 2 | e^{-d\beta \hat{H}} | 3 \rangle \langle 3 | e^{-d\beta \hat{H}} | 1 \rangle, \text{ contribution} = (-1)^3 d\beta^3. \quad (23)$$

However, frustration does not necessarily mean there must be a sign problem. Clever choice of basis and make the QMC simulation sign-problem free. As discussed in Sec. 3.2, there is no sign problem for some bilayer frustrated models [19, 20, 21, 22, 23]. Inspired by these works and considering the model that has the same ground state as the above model, one can extend the simulation basis from spin to singlet-triplet or even plaquette bases, and recently there are progresses in such cases by means of changing the simulation basis from spin to bond or even plaquette [24, 25] to reduce the sign problem in the QMC simulation for 2D antiferromagnetic Shastry-Sutherland spin model.

4.4. Sign Problem is related to Aharonov-Anandan Phase

For DQMC, the sign problem is thought to be related to topological properties of the configurations [12]. One can define the weight as:

$$W(C_i) = \det \left[1 + e^{\beta\mu} \mathcal{T} \exp \int_0^\beta d\tau H^{\text{aux}}[C_i(\tau)] \right], \quad (24)$$

then define

$$G(\tau; \beta) = \mathcal{T} \exp \int_\tau^{\tau+\beta} d\tau' H^{\text{aux}}[C_i(\tau')], \quad (25)$$

the corresponding eigenvalue and eigenstate are: $G(\tau; \beta) |\phi_n(\tau)\rangle = \lambda_n |\phi_n(\tau)\rangle$.

Now one finds the weight is

$$W(C_i) = \prod_n \left(1 + \lambda_n e^{\beta\mu} \right) \quad (26)$$

by defining $\lambda_n = e^{i\theta_n} \omega_n$ and $e^{i\theta_n} = \prod_{\tau=0}^\beta \langle \phi_n(\tau + d\tau) | \phi_n(\tau) \rangle$. These phases $e^{i\theta_n}$ are imaginary time versions of the Aharonov-Anandan (AA) phase. If we take $\beta \rightarrow \infty$, which means the adiabatic limit, then the eigenstate $|\psi_n(\tau)\rangle = \lim_{\beta \rightarrow \infty} |\phi_n(\tau)\rangle$ and the weights is $\exp \left[- \int_0^\beta \varepsilon_n(\tau) d\tau \right]$, where $\varepsilon_n(\tau)$ is eigenvalue of $H^{\text{aux}}(\tau)$. Now $e^{i\theta_n}$ becomes a Berry phase of the instantaneous eigenstates $|\phi_n(\tau)\rangle$.

This analogy gives us a new perspective on the sign problem, but it doesn't help to mitigate it. In the next Section, we will discuss understanding and practical implementation scheme to cure, ease and make use of the sign problem.

5. How to cure, ease and make use of the sign problem

How to reduce the exponential computation complexity introduced by the sign problem, there is no general methods, and there are different solutions for different physical systems. We note only the recent *Sign bound theory* has pointed out a generic direction [33]. Below, we select few important cases and explain their usages.

5.1. Symmetry

In DQMC for interacting fermion models, where $H = H_K + H_I$, H_K is kinetic energy part and H_I is the part of the interaction after decoupling [26], if there exists an anti-unitary operator T , such that

$$T H_K T^{-1} = H_K, \quad T H_I T^{-1} = H_I, \quad T^2 = -1 \quad (27)$$

then for the eigenvalues λ_i of matrix $I + B(\beta, 0)$, where $B(\beta, 0)$ is defined in Eq. (15). We know $\prod \lambda_i$ is real and positive number.

The proof is simple. If $(I + B) |\Psi_i\rangle = \lambda_i |\Psi_i\rangle$ then $T |\Psi_i\rangle$ is also eigenstate of matrix $(I + B)$ with eigenvalue λ_i^* . That is, the eigenvalues of λ_i and λ_i^* come in pairs, and the weight $\det(I + B) = \prod |\lambda_i|^2 \geq 0$. The orthogonality of the two eigenstates is trivial: $\langle \Psi_i | T \Psi_i \rangle = \langle \Psi_i | T^\dagger T T |\Psi_i\rangle^* = -\langle \Psi_i | T^\dagger |\Psi_i\rangle^* = -\langle T \Psi_i | \Psi_i \rangle^* = -\langle \Psi_i | T \Psi_i \rangle = 0$. The overlap of the two states is zero.

In practice, one usually divides the configurational weight of the original problem into two parts according to the degrees of freedom, such as the spin up and down, then perform a unitary transformation to show the two parts of the weights are either the same real number or complex conjugate with each other, such as their products is positive definite. For example, Hubbard Model at half filling, if $U > 0$, $e^{-\Delta\tau \hat{H}_U} = \gamma \sum_{s=\pm 1} e^{\alpha s (\hat{n}_\uparrow + \hat{n}_\downarrow - 1)}$ where $\gamma = \frac{1}{2} e^{\Delta\tau U/4}$, $\cosh(\alpha) = e^{-\Delta\tau U/2}$, and α is an imaginary number. Now the unitary transformation is the particle-hole transformation,

$$\begin{cases} \hat{c}_{i\downarrow}^\dagger \rightarrow (-1)^i \hat{c}_{i\downarrow} \\ \hat{c}_{i\downarrow} \rightarrow (-1)^i \hat{c}_{i\downarrow}^\dagger \end{cases} \quad (28)$$

then

$$\alpha \text{ is an imaginary number} \rightarrow \begin{cases} \alpha (\hat{n}_{i\uparrow} + \hat{n}_{i\downarrow} - 1) \xrightarrow{PH \text{ for spin-down}} \alpha s_i (\hat{n}_{i\uparrow} - \hat{n}_{i\downarrow}) \\ e^{\alpha s_i (\hat{n}_{i\uparrow} + \hat{n}_{i\downarrow} - 1)} \xrightarrow{PH \text{ for spin-down}} e^{\alpha s_i (\hat{n}_{i\uparrow} - \hat{n}_{i\downarrow})} \end{cases} \quad (29)$$

Since α is an imaginary number, it's clear to see that after such a particle-hole transformation, spin up and down parts are complex conjugated to each other.

In addition to particle-hole symmetry, other symmetries such as $C_2T + C_2P$ symmetries [30, 31] may also make the system sign-free. In short, we want to find an anti-unitary transformation that makes the system invariant, or to apply a unitary transformation, then the weights are divided into two parts that are obviously complex conjugate to each other. Such scheme has been widely used in the DQMC solution of interaction driven topological phase transitions, such as in Kane-Mele Hubbard model [86, 87].

5.2. Split Orthogonal Group, Majorana representation and Majorana Positivity

Subsequently, people have made more in-depth studies on sign of determinants of matrices. For example, there is a theorem[38] :

If M belongs to the split orthogonal group $O(n, n)$, then :

$$\det(I + M) \begin{cases} \geq 0, & \text{if } M \in O^{++}(n, n), \\ \leq 0, & \text{if } M \in O^{--}(n, n), \\ 0, & \text{otherwise.} \end{cases} \quad (30)$$

where the split orthogonal group $O(n, n)$ is formed by all $2n \times 2n$ real matrices that preserve the metric $\eta = \text{diag}(\underbrace{1, \dots, 1}_n, \underbrace{-1, \dots, -1}_n)$, $M^T \eta M = \eta$. Split orthogonal group $O(n, n)$ means that if we write the matrix M in the block form like: $M = \begin{pmatrix} M_{11} & M_{12} \\ M_{21} & M_{22} \end{pmatrix}$, then we have $|\det(M_{11})| \geq 1$ and $|\det(M_{22})| \geq 1$. And we use the notation $O^{\pm\pm}(n, n)$ to classified the four components of $O(n, n)$ by considering the signs of $\det(M_{11})$ and $\det(M_{22})$.

Since the fermion sign problem is related to the basis of decoupling, it can be found that some models translated to Majorana representation are sign-problem free [34, 35, 36]. Majorana representation is turning fermions into Majorana fermions:

$$\hat{c}_i = \frac{1}{2} (\gamma_i^1 + i\gamma_i^2), \quad \hat{c}_i^\dagger = \frac{1}{2} (\gamma_i^1 - i\gamma_i^2) \quad (31)$$

These findings inspired research on Majorana reflection positivity or the Majorana Kramers positivity [37]. One can write the H_0 and decoupled Hamiltonian under the Majorana representation: $H_{bl} = \gamma^T V \gamma$. Then

(a) if V is a Majorana reflection positive kernel, which means it can be represented as

$$V = \begin{pmatrix} A & iB \\ -iB^T & A^* \end{pmatrix} \quad (32)$$

where A and B are $N \times N$ matrices. A is complex antisymmetric matrix and B is a Hermitian matrix. Or,

(b) if there exist two transformation operators S and P such that

$$\begin{aligned} S^T V S &= V^*, \\ P V P^{-1} &= V, \end{aligned} \quad (33)$$

where S is a real antisymmetric matrix and P is a symmetric or antisymmetric Hermitian matrix, and we need P anticommutes with S . There is no sign problem in the DQMC simulation.

In Ref. [88], there is a similar discussion on the sign problem related with the structure of the fermion determinant. It is proved that if $D \in \text{SU}(n, m)$, then $\det(I_{n+m} + D) \in \mathbb{R}$, where $\text{SU}(n, m)$ is a pseudounitary group. Such condition is used to guarantee the DQMC simulation for $U(1)$ gauge field coupled to Dirac fermions in $(2+1)\text{d}$, a fundamental problem for both high-energy physics and condensed matter physics related to quantum electrodynamics and deconfined quantum criticalities, is sign-problem free [88, 89, 90].

5.3. Sign bound theory

As discussed in Sec. 4, for systems with sign problems, we can usually sample them by reweighting and the average sign is usually $\langle s \rangle = Z/Z' \sim e^{-\beta N \Delta f}$. However, the difference of free energy Δf between the reference system Z' and the system Z is not necessarily a constant with little change, but may be a quantity depending on the system size $N = L^d$ and inverse temperature $\beta = \frac{1}{k_B T}$.

In some systems, we find that in the zero temperature limit, the sign does not decay exponentially with respect to size L but rather decay algebraically [32, 33], implying that Δf could be a logarithmic function of L .

In fact, in the zero temperature limit, the mean of the signs is $\langle s \rangle_R = \frac{Z}{Z^R} = \frac{g e^{-\beta E_0}}{g^R e^{-\beta E_0^R}}$, as given in Eq. (19). We can choose a good reference system Z^R , which have same ground state energy $E_0^R = E_0$ with Z . Then the mean of the signs is $\langle s \rangle_R = g/g^R$, which is only related to the ratio of ground state degeneracy. And as shown in the cases below, in a few common cases, such as the lattice model for quantum Moiré materials in momentum space [30, 67, 33, 68] and extended Hubbard model in real space [32, 65, 66, 63], the ground state degeneracy is a polynomial function of the size of the system.

Even if most of the time we can not find such a perfect Z^R , we can still consider the upper bound on the value of Z^R , which means if we know $Z^R \leq C$, then in the zero temperature limit we can get a lower bound of the sign: $\langle s \rangle_R = \frac{Z}{Z^R} \geq \frac{g e^{-\beta E_0}}{C}$. This is the *Sign bound theory* [33]. Two cases of the theory will be shown below. In case 1: $Z^R = g^R e^{-\beta E_0^R} \leq \sqrt{g' e^{-\beta E_0'}} e^{-\beta E_0}$ and $E_0'/2 = E_0$ such that $\langle s \rangle_R = \frac{Z}{Z^R} \geq \frac{g e^{-\beta E_0}}{\sqrt{g' e^{-\beta E_0'}} e^{-\beta E_0}} = g/\sqrt{g'} e^{-\beta(E_0 - E_0'/2)} = g/\sqrt{g'}$, and in case 2: $Z^R = g^R e^{-\beta E_0^R} \leq g' e^{-\beta E_0'}$ and $E_0' = E_0$ such that $\langle s \rangle_R = \frac{Z}{Z^R} \geq \frac{g e^{-\beta E_0}}{g' e^{-\beta E_0}} = g/g' e^{-\beta(E_0 - E_0')} = g/g'$. If we succeed in finding such an upper bound on Z^R which can cancel out $e^{-\beta E_0}$ term in the denominator, then the lower bound of the sign is just a function of the ground state degeneracy. If the ground state degeneracy is a polynomial function of the size of the system, then we can obtain a lower bound of the average sign algebraically decay with the system size.

5.3.1. Case 1

For example, we choose $Z^R = \sum_{\{l\}} P(\{l\}) |\mathcal{R}(D(\{l\}))| \equiv \langle |\mathcal{R}(D)| \rangle$ and $Z' = \sum_{\{l\}} P(\{l\}) |D|^2(\{l\}) \equiv \langle |D|^2 \rangle$, where $Z = \sum_{\{l\}} P(\{l\}) D(\{l\}) \equiv \langle D \rangle = \langle \mathcal{R}(D) \rangle$. Here $D(\{l\})$ is the determinant term in weight, and $P(\{l\})$ is a normalized probability distribution. Because $\langle |\mathcal{R}(D)| \rangle \leq \sqrt{\langle |D|^2 \rangle}$ then $\langle s \rangle = \frac{Z}{Z^R} \geq \frac{g e^{-\beta E_0}}{\sqrt{g' e^{-\beta E_0'}} e^{-\beta E_0}} = g/\sqrt{g'} e^{-\beta(E_0 - E_0'/2)} = g/\sqrt{g'}$, if $E_0'/2 = E_0$.

The twisted-bilayer-graphene(TBG) models, projected to the flat bands, belong to such a case [30, 67]. In the chiral limit, the Hamiltonian only has density-density interaction in momentum space

$$H = \sum_{q \neq 0} V(q) \rho_{-q} \rho_q = \sum_{q \neq 0} V(q) \rho_q^\dagger \rho_q \quad (34)$$

where $\rho_q = \sum_{i,j} (\lambda_{i,j}(q) \hat{c}_i^\dagger c_j - \frac{1}{2} \mu_q)$.

If we set λ is random number and $\mu_q = 0$, and there is no other symmetry, then $E_0 = E_0'/2$. For ground state degeneracy, it's easy to know $g = 2$ and $g' = N + 3$, by introducing a raising operator $\Delta^\dagger = \sum_{i'} c_{i',+}^\dagger c_{i',-}$. Then at low temperature, $\langle s \rangle \geq 2/\sqrt{N+3}$ (as shown in Fig. 5 (a)).

We consider single valley/spin two band $(m, n \in \{1, -1\})$ TBG model at half-filling and chiral limit, which means $\lambda_{i,j,m,n}(q) = m \cdot n \cdot \lambda_{i,j,m,n}(q)$ and $\mu_q \neq 0$. Similarly, we still have $E_0 = E_0'$ and $g = 2$, and now $g' = (N+1)^2 + 2$. Then at low temperature, $\langle s \rangle \geq 2/\sqrt{(N+1)^2 + 2}$ (as shown in Fig. 5 (b)).

5.3.2. Case 2

If we consider the real space extended Hubbard model [32, 65, 66], which also offer the description of the TBG systems once the interactions are projected to the flat bands with truncation:

$$\hat{H} = U \sum_{\square} (\hat{Q}_{\square} + \alpha \hat{T}_{\square} - \nu)^2 \quad (35)$$

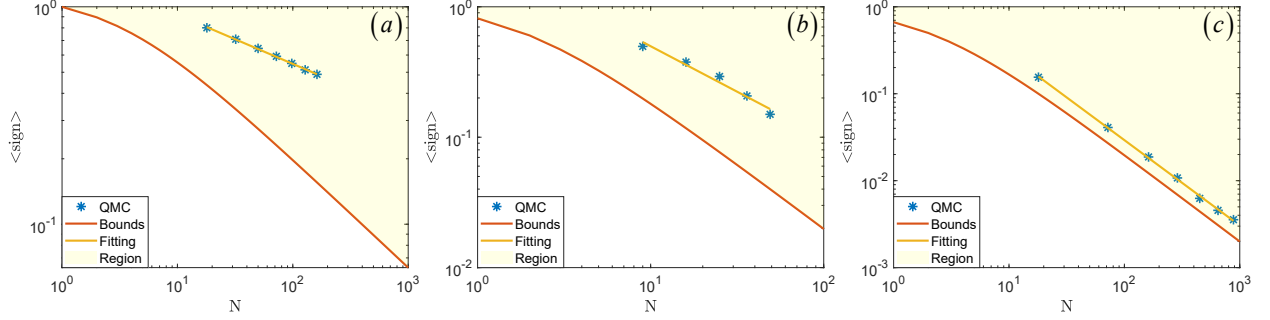


Figure 5: The average sign for three different cases according to the *sign bound theory*. All measurement are carried out at an average sign converged temperature. The errors in QMC data are smaller than the symbol size. (a) momentum space case, now λ is randomly set, and the red line gives us the lower bound $\langle s \rangle \geq 2/\sqrt{N+3}$. Here $N = 18, 32, 50, 72, 98, 128, 162$. Fitting line $\propto N^{-0.23}$. (b) momentum space case, we consider $\nu = 0$ single valley/spin TBG model in chiral limit, and the red line gives us the lower bound $\langle s \rangle \geq 2/\sqrt{(N+1)^2+2}$. $N = 9, 16, 25, 36, 49$ and $T = 0.91$ meV. Fitting line $\propto N^{-0.70}$. (c) For real space TBG model, the red line lower bound is $\langle s \rangle \geq 2/(N+2)$ and $N = 18, 72, 162, 288, 450, 648, 882$. The parameters of QMC are detailed in [32]. Fitting line $\propto N^{-0.98}$.

where $\hat{Q}_\square = \frac{1}{3} \sum_{\sigma, \tau} \sum_{l=1}^6 \hat{c}_{R+\delta_l, \sigma, \tau}^\dagger \hat{c}_{R+\delta_l, \sigma, \tau} - 4$, $\hat{T}_\square = \sum_{\sigma, \tau} \sum_{l=1}^6 [(-1)^l \hat{c}_{R+\delta_{l+1}, \sigma, \tau}^\dagger \hat{c}_{R+\delta_l, \sigma, \tau} + \text{h.c.}]$, ν is used to control filling, σ, τ are spin and valley indexes, $R + \delta_l$ represents site l in a single R hexagon and U, α is real number coming from the overlap of Wannier functions on the Moiré scale.

Here, we choose $Z' = \sum_{\{l\}} P(\{l\}) |D(\{l\})| \equiv \langle |D| \rangle$, still $Z^R = \sum_{\{l\}} P(\{l\}) |\mathcal{R}(D(\{l\}))| \equiv \langle |\mathcal{R}(D)| \rangle$ and $Z = \sum_{\{l\}} P(\{l\}) D(\{l\}) \equiv \langle D \rangle = \langle \mathcal{R}(D) \rangle$. Because $\langle |\mathcal{R}(D)| \rangle \leq \langle |D| \rangle$ then $\langle s \rangle = \frac{Z}{Z^R} \geq \frac{g e^{-\beta E_0}}{g' e^{-\beta E'_0}} = g/g' e^{-\beta(E_0 - E'_0)} = g/g'$. Similarly, we still have $E'_0 = E_0$. It can be computed from tensor Young tableau method that, at $\nu = \pm 2$, $g = (N+3)(N+2)(N+1)/6$, and at $\nu = 0$, $g' = (N+3)(N+2)^2(N+1)/12$ [33]. Then at low temperature, $\langle s \rangle \geq g/g' = 2/(N+2)$ (as shown in Fig. 5 (c)).

For the model we mentioned above and its reference system, the exponential decay part cancels out, and we can easily calculate the ground state degeneracy. As shown in Fig. 5, numerically we also see that at very low temperatures, the average sign is polynomial decay.

5.4. Lefschetz thimble

This is also a method that can be used to cure or reduce the sign problem in lattice fermion QMC simulations [49, 50, 91, 92, 93, 94, 95, 96, 97], here we only briefly outline its main idea.

For computing expectation value $\langle O[x] \rangle$ in Monte Carlo sampling on the configuration space $[x]$, we have

$$\begin{aligned} \langle O[x] \rangle &= \frac{1}{Z} \int dx e^{-S[x]} O[x] \\ &= \frac{\int dx e^{-S_R[x]} e^{-iS_I[x]} O[x]}{\int dx e^{-S_R[x]} e^{-iS_I[x]}} \\ &= \frac{\int dx e^{-S_R[x]} e^{-iS_I[x]} O[x]}{\int dx e^{-S_R[x]}} \bigg/ \frac{\int dx e^{-S_R[x]} e^{-iS_I[x]}}{\int dx e^{-S_R[x]}} \\ &= \frac{\langle e^{-iS_I} O \rangle_R}{\langle e^{-iS_I} \rangle_R} \end{aligned} \quad (36)$$

where R and I means real and imaginary parts of action $S[x]$. And $\langle \cdot \rangle_R$ is defined as $\langle O \rangle_R = \frac{\int dx e^{-S_R[x]} O}{\int dx e^{-S_R[x]}}$.

If action $S[x]$ is analytic for all $x \in \mathbb{C}^n$, its saddle points are nondegenerate and Eq. (36) is convergent, then Morse theory [98, 99, 100] told us these integrals can be evaluated using the steepest descent cycles \mathcal{J}_σ and they are called Lefschetz thimbles, which means we can replace the integration over the real domain R^n with that over curved complex n -dimensional manifolds \mathcal{J}_σ

$$\int_{\mathbb{R}^n} d^n x e^{-S(x)} = \sum_{\sigma} n_{\sigma} \int_{\mathcal{J}_{\sigma}} d^n z e^{-S(z)} \quad (37)$$

where the Lefschetz thimbles \mathcal{J}_σ are the union of all solutions of the gradient flow equations:

$$\frac{dz(\tau)}{d\tau} = -\frac{\overline{\partial S}}{\partial z} \quad (38)$$

and it start from the corresponding saddle point z_σ , which means $\lim_{\tau \rightarrow \infty} z(\tau) = z_\sigma$. Here σ is the index for different saddle point/Lefschetz thimbles, τ is a parameter and the overline represents complex conjugation, and saddle point is the point on the surface of S where the derivatives in orthogonal directions are all zero, but is not a local extremum. While the thimbles always end inside regions of stability, duals thimbles(anti-thimbles) \mathcal{K}_σ are also such solutions at a given saddle point $\lim_{\tau \rightarrow -\infty} z(\tau) = z_\sigma$ and end inside regions of instability. We can make an analogy between the dual thimble and the contour of steepest ascent, as we did with thimble and the contour of steepest descent. And n_σ are intersection numbers (which decides the contribution of a particular saddle point z_σ to the partition function) of hypersurface generated by the paths of steepest ascent duals \mathcal{K}_σ and original region of integration \mathbb{R} :

$$n_\sigma = \langle \mathcal{K}_\sigma, \mathbb{R}^n \rangle \quad (39)$$

The important point of such construction is: $\text{Im}[S]$ is constant on Lefschetz thimbles (mod 2π), which means there is no sign problem on each thimble. The ratio of weights in the same thimble must be a positive real number, since the phase of the weight is the same.

Let's take a trivial 1d case for the purpose of illustration[101, 102]:

$$\int_{\mathbb{R}+i\varepsilon} dx \frac{1}{x} e^{-x^2/2} = \sum_\sigma n_\sigma \int_{\mathcal{J}_\sigma} dz e^{-S(z)} \quad (40)$$

which corresponds to the case $S[z] = \log z + z^2/2$. The two critical points of this action are: $z_1 = i$, $z_2 = -i$. Since we know that the imaginary parts $\text{Im}[S]$ are constant on Lefschetz thimbles, then we have: $\text{Im}(S[z])|_{\text{along } \mathbb{R}+i\varepsilon} = \text{Im} S[z_\sigma] = \pm i\pi/2$. Following the procedure described above we can obtain the corresponding thimbles and dual thimbles(as shown in Fig. 6), and then: $\int_{\mathbb{R}+i\varepsilon} dx \frac{1}{x} e^{-x^2/2} = \int_{\mathcal{J}_1} dz e^{-S(z)}$.

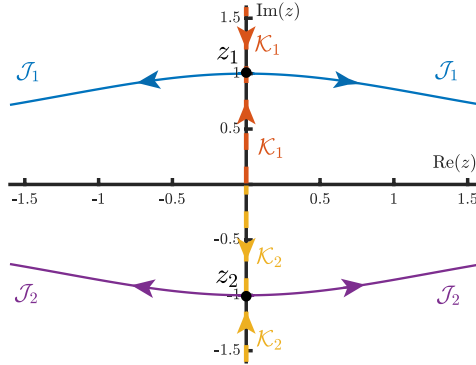


Figure 6: A schematic plot of thimbles and dual thimbles. Here the black dots are saddle points $z_{1,2}$, while the solid blue/purple lines correspond to thimbles and the dotted red/yellow lines correspond to dual thimbles. And the arrows show the directions of the flows. See intersection numbers of dual thimbles and $\mathbb{R} + i\varepsilon$, we know $n_1 = 1$, $n_2 = 0$.

The Lefschetz thimbles method is commonly used to calculate the value of certain integrals and in high-energy physics and real time calculations. Recently with the application of hybrid Monte Carlo in condensed matter, there has been a lot of work using Lefschetz thimbles method to study common condensed matter problems which has sign problem. For example, Hubbard model on the hexagonal(honeycomb) lattice at finite chemical potential with linear system size $L = 6$ and inverse temperature $\beta = 20$, has been successfully simulated with Lefschetz thimbles method in DQMC [49, 97].

6. Conclusion

In this article, we give a pedagogical overview on the origin of the sign problem in various quantum Monte Carlo simulation techniques, ranging from the world-line and stochastic series expansion Monte Carlo for boson and spin systems to the determinant and momentum space quantum Monte Carlo for interacting fermions. We have elaborated on the definition of the sign problem and its possible origins, including Pauli exclusion principle, geometric frustration and the lack of symmetry requirements, etc. In addition, we also point out the sign problem is actually basis-dependent and summarizes established ways to ensure that some models are free of sign problems such as checking symmetry and Majorana positivity. We explain what to do when there is sign problem in general: reweighting, and how to reduce the severity of sign problems, in particular that based on the properties of the finite size partition functions, the recent *sign bound theory* could distinguish when the bounds have the usual exponential scaling, and when they are bestowed with an algebraic scaling at low temperature limit. Fermionic QMC simulations with such algebraic sign problems have been successfully carried out for extended Hubbard-type and quantum Moiré lattice models.

Acknowledgement

We thank Xu Zhang, Weilun Jiang, Yuan Da Liao and Xiao Yan Xu for insightful discussions and fruitful collaborations on related topics over the years. GPP and ZYM acknowledge the support from the Research Grants Council of Hong Kong SAR of China (Grant Nos. 17303019, 17301420, 17301721 and AoE/P-701/20), the Strategic Priority Research Program of the Chinese Academy of Sciences (Grant No. XDB33000000), the K. C. Wong Education Foundation (Grant No. GJTD-2020-01) and the Seed Funding “QuantumInspired explainable-AI” at the HKU-TCL Joint Research Centre for Artificial Intelligence. We thank the Information Technology Services at the University of Hong Kong and the Tianhe platforms at the National Supercomputer Centers for their technical support and generous allocation of CPU time.

References

- [1] W. M. C. Foulkes, L. Mitás, R. J. Needs, and G. Rajagopal. Quantum monte carlo simulations of solids. *Rev. Mod. Phys.*, 73:33–83, Jan 2001.
- [2] J. Carlson, S. Gandolfi, F. Pederiva, Steven C. Pieper, R. Schiavilla, K. E. Schmidt, and R. B. Wiringa. Quantum monte carlo methods for nuclear physics. *Rev. Mod. Phys.*, 87:1067–1118, Sep 2015.
- [3] F.F. Assaad and H.G. Evertz. *World-line and Determinantal Quantum Monte Carlo Methods for Spins, Phonons and Electrons*, pages 277–356. Springer Berlin Heidelberg, Berlin, Heidelberg, 2008.
- [4] Anders W. Sandvik. Computational studies of quantum spin systems. *AIP Conference Proceedings*, 1297(1):135–338, 2010.
- [5] Xiao Yan Xu, Zi Hong Liu, Gaopei Pan, Yang Qi, Kai Sun, and Zi Yang Meng. Revealing fermionic quantum criticality from new monte carlo techniques. *Journal of Physics: Condensed Matter*, 31(46):463001, aug 2019.
- [6] E. Y. Loh, J. E. Gubernatis, R. T. Scalettar, S. R. White, D. J. Scalapino, and R. L. Sugar. Sign problem in the numerical simulation of many-electron systems. *Phys. Rev. B*, 41:9301–9307, May 1990.
- [7] Matthias Troyer and Uwe-Jens Wiese. Computational complexity and fundamental limitations to fermionic quantum monte carlo simulations. *Phys. Rev. Lett.*, 94:170201, May 2005.
- [8] Ribhu K Kaul, Roger G Melko, and Anders W Sandvik. Bridging lattice-scale physics and continuum field theory with quantum monte carlo simulations. *Annu. Rev. Condens. Matter Phys.*, 4(1):179–215, 2013.
- [9] Masako Takasu, Seiji Miyashita, and Masuo Suzuki. Monte Carlo Simulation of Quantum Heisenberg Magnets on the Triangular Lattice. *Progress of Theoretical Physics*, 75(5):1254–1257, 05 1986.
- [10] Naomichi Hatano and Masuo Suzuki. Representation basis in quantum monte carlo calculations and the negative-sign problem. *Physics Letters A*, 163(4):246–249, 1992.
- [11] J. E. Hirsch. Two-dimensional hubbard model: Numerical simulation study. *Phys. Rev. B*, 31:4403–4419, Apr 1985.
- [12] Mauro Iazzi, Alexey A. Soluyanov, and Matthias Troyer. Topological origin of the fermion sign problem. *Phys. Rev. B*, 93:115102, Mar 2016.
- [13] R. Mondaini, S. Tarat, and R. T. Scalettar. Quantum critical points and the sign problem. *Science*, 375(6579):418–424, 2022.
- [14] S. Tarat, Bo Xiao, R. Mondaini, and R. T. Scalettar. Deconvolving the components of the sign problem. *Phys. Rev. B*, 105:045107, Jan 2022.
- [15] MB Hastings. How quantum are non-negative wavefunctions? *Journal of Mathematical Physics*, 57(1):015210, 2016.
- [16] Zohar Ringel and Dmitry L Kovrizhin. Quantized gravitational responses, the sign problem, and quantum complexity. *Science advances*, 3(9):e1701758, 2017.
- [17] Adam Smith, Omri Golan, and Zohar Ringel. Intrinsic sign problems in topological quantum field theories. *Phys. Rev. Research*, 2:033515, Sep 2020.
- [18] Omri Golan, Adam Smith, and Zohar Ringel. Intrinsic sign problem in fermionic and bosonic chiral topological matter. *Phys. Rev. Research*, 2:043032, Oct 2020.

- [19] Fabien Alet, Kedar Damle, and Sumiran Pujari. Sign-problem-free monte carlo simulation of certain frustrated quantum magnets. *Phys. Rev. Lett.*, 117:197203, Nov 2016.
- [20] Kwai-Kong Ng and Min-Fong Yang. Field-induced quantum phases in a frustrated spin-dimer model: A sign-problem-free quantum monte carlo study. *Phys. Rev. B*, 95:064431, Feb 2017.
- [21] A. Honecker, S. Wessel, R. Kerkdyk, T. Pruschke, F. Mila, and B. Normand. Thermodynamic properties of highly frustrated quantum spin ladders: Influence of many-particle bound states. *Phys. Rev. B*, 93:054408, Feb 2016.
- [22] J. Stapmanns, P. Corboz, F. Mila, A. Honecker, B. Normand, and S. Wessel. Thermal critical points and quantum critical end point in the frustrated bilayer heisenberg antiferromagnet. *Phys. Rev. Lett.*, 121:127201, Sep 2018.
- [23] Stefan Wessel, B. Normand, Frédéric Mila, and Andreas Honecker. Efficient Quantum Monte Carlo simulations of highly frustrated magnets: the frustrated spin-1/2 ladder. *SciPost Phys.*, 3:005, 2017.
- [24] Stefan Wessel, Ido Niesen, Jonas Stapmanns, B. Normand, Frédéric Mila, Philippe Corboz, and Andreas Honecker. Thermodynamic properties of the shastry-sutherland model from quantum monte carlo simulations. *Phys. Rev. B*, 98:174432, Nov 2018.
- [25] Jonathan D’Emidio, Stefan Wessel, and Frédéric Mila. Reduction of the sign problem near $t = 0$ in quantum monte carlo simulations. *Phys. Rev. B*, 102:064420, Aug 2020.
- [26] Congjun Wu and Shou-Cheng Zhang. Sufficient condition for absence of the sign problem in the fermionic quantum monte carlo algorithm. *Phys. Rev. B*, 71:155115, Apr 2005.
- [27] G. H. Lang, C. W. Johnson, S. E. Koonin, and W. E. Ormand. Monte carlo evaluation of path integrals for the nuclear shell model. *Phys. Rev. C*, 48:1518–1545, Oct 1993.
- [28] S.E. Koonin, D.J. Dean, and K. Langanke. Shell model monte carlo methods. *Physics Reports*, 278(1):1–77, 1997.
- [29] S. Hands, I. Montvay, S. Morrison, M. Oevers, L. Scorzato, and J. Skullerud. Numerical study of dense adjoint matter in two color qcd. *The European Physical Journal C - Particles and Fields*, 17(2):285–302, 2000.
- [30] Xu Zhang, Gaopei Pan, Yi Zhang, Jian Kang, and Zi Yang Meng. Momentum space quantum monte carlo on twisted bilayer graphene. *Chinese Physics Letters*, 38(7):077305, 2021.
- [31] Johannes S Hofmann, Eslam Khalaf, Ashvin Vishwanath, Erez Berg, and Jong Yeon Lee. Fermionic monte carlo study of a realistic model of twisted bilayer graphene. *arXiv preprint arXiv:2105.12112*, 2021.
- [32] Yunqing Ouyang and Xiao Yan Xu. Projection of infinite- u hubbard model and algebraic sign structure. *Phys. Rev. B*, 104:L241104, Dec 2021.
- [33] Xu Zhang, Gaopei Pan, Xiao Yan Xu, and Zi Yang Meng. Sign problem finds its bounds. *arXiv preprint arXiv:2112.06139*, 2021.
- [34] Zi-Xiang Li, Yi-Fan Jiang, and Hong Yao. Solving the fermion sign problem in quantum monte carlo simulations by majorana representation. *Phys. Rev. B*, 91:241117, Jun 2015.
- [35] Zi-Xiang Li, Yi-Fan Jiang, and Hong Yao. Majorana-time-reversal symmetries: A fundamental principle for sign-problem-free quantum monte carlo simulations. *Phys. Rev. Lett.*, 117:267002, Dec 2016.
- [36] Zi-Xiang Li and Hong Yao. Sign-problem-free fermionic quantum monte carlo: Developments and applications. *Annual Review of Condensed Matter Physics*, 10(1):337–356, 2019.
- [37] Z. C. Wei, Congjun Wu, Yi Li, Shiwei Zhang, and T. Xiang. Majorana positivity and the fermion sign problem of quantum monte carlo simulations. *Phys. Rev. Lett.*, 116:250601, Jun 2016.
- [38] Lei Wang, Ye-Hua Liu, Mauro Iazzi, Matthias Troyer, and Gergely Harcos. Split orthogonal group: A guiding principle for sign-problem-free fermionic simulations. *Phys. Rev. Lett.*, 115:250601, Dec 2015.
- [39] Hiroshi Shinaoka, Yusuke Nomura, Silke Biermann, Matthias Troyer, and Philipp Werner. Negative sign problem in continuous-time quantum monte carlo: Optimal choice of single-particle basis for impurity problems. *Phys. Rev. B*, 92:195126, Nov 2015.
- [40] Ryan Levy and Bryan K. Clark. Mitigating the sign problem through basis rotations. *Phys. Rev. Lett.*, 126:216401, May 2021.
- [41] Giacomo Torlai, Juan Carrasquilla, Matthew T. Fishman, Roger G. Melko, and Matthew P. A. Fisher. Wave-function positivization via automatic differentiation. *Phys. Rev. Research*, 2:032060, Sep 2020.
- [42] Dominik Hangleiter, Ingo Roth, Daniel Nagaj, and Jens Eisert. Easing the monte carlo sign problem. *Science Advances*, 6(33):eabb8341, 2020.
- [43] Joel Klassen, Milad Marvian, Stephen Piddock, Marios Ioannou, Itay Hen, and Barbara M Terhal. Hardness and ease of curing the sign problem for two-local qubit hamiltonians. *SIAM Journal on Computing*, 49(6):1332–1362, 2020.
- [44] Milad Marvian, Daniel A Lidar, and Itay Hen. On the computational complexity of curing non-stoquastic hamiltonians. *Nature communications*, 10(1):1–9, 2019.
- [45] Aaram J. Kim, Philipp Werner, and Roser Valentí. Alleviating the sign problem in quantum monte carlo simulations of spin-orbit-coupled multiorbital hubbard models. *Phys. Rev. B*, 101:045108, Jan 2020.
- [46] Riccardo Rossi. Determinant diagrammatic monte carlo algorithm in the thermodynamic limit. *Phys. Rev. Lett.*, 119:045701, Jul 2017.
- [47] R. Rossi, N. Prokof’ev, B. Svistunov, K. Van Houcke, and F. Werner. Polynomial complexity despite the fermionic sign. *EPL (Europhysics Letters)*, 118(1):10004, 2017.
- [48] Jonathan D’Emidio, Stefan Wessel, and Frédéric Mila. Reduction of the sign problem near $t = 0$ in quantum monte carlo simulations. *Phys. Rev. B*, 102:064420, Aug 2020.
- [49] Maksim Ulybyshev, Christopher Winterowd, and Savvas Zafeiropoulos. Lefschetz thimbles decomposition for the hubbard model on the hexagonal lattice. *Phys. Rev. D*, 101:014508, Jan 2020.
- [50] Andrei Alexandru, Gokce Basar, Paulo F Bedaque, and Neill C Warrington. Complex paths around the sign problem. *arXiv preprint arXiv:2007.05436*, 2020.
- [51] S. Chandrasekharan and U. J. Wiese. Meron-cluster solution of fermion sign problems. *Physical Review Letters*, 83(16):3116–3119, 1999.
- [52] Emilie Fulton Huffman and Shailesh Chandrasekharan. Solution to sign problems in half-filled spin-polarized electronic systems. *Phys. Rev. B*, 89:111101, Mar 2014.
- [53] Zhong-Chao Wei. Semigroup approach to the sign problem in quantum monte carlo simulations. *arXiv preprint arXiv:1712.09412*, 2017.
- [54] Xiao Yan Xu, Yang Qi, Long Zhang, Fakher F. Assaad, Cenke Xu, and Zi Yang Meng. Monte carlo study of lattice compact quantum

- electrodynamics with fermionic matter: The parent state of quantum phases. *Phys. Rev. X*, 9:021022, May 2019.
- [55] Zhou-Quan Wan, Shi-Xin Zhang, and Hong Yao. Mitigating sign problem by automatic differentiation. *arXiv preprint arXiv:2010.01141*, 2020.
- [56] Peter Broecker, Juan Carrasquilla, Roger G Melko, and Simon Trebst. Machine learning quantum phases of matter beyond the fermion sign problem. *Scientific reports*, 7(1):1–10, 2017.
- [57] Jan-Lukas Wynen, Evan Berkowitz, Stefan Krieg, Thomas Luu, and Johann Ostmeyer. Machine learning to alleviate hubbard-model sign problems. *Phys. Rev. B*, 103:125153, Mar 2021.
- [58] Mohammad-Sadegh Vaezi, Amir-Reza Negari, Amin Moharramipour, and Abolhassan Vaezi. Amelioration for the sign problem: An adiabatic quantum monte carlo algorithm. *Phys. Rev. Lett.*, 127:217003, Nov 2021.
- [59] Scott Lawrence. Perturbative removal of a sign problem. *Phys. Rev. D*, 102:094504, Nov 2020.
- [60] V. I. Iglovikov, E. Khatami, and R. T. Scalettar. Geometry dependence of the sign problem in quantum monte carlo simulations. *Phys. Rev. B*, 92:045110, Jul 2015.
- [61] S. Tarat, Bo Xiao, R. Mondaini, and R. T. Scalettar. Deconvolving the components of the sign problem. *Phys. Rev. B*, 105:045107, Jan 2022.
- [62] Eduardo Ibarra-García-Padilla, Sohail Dasgupta, Hao-Tian Wei, Shintaro Taie, Yoshiro Takahashi, Richard T. Scalettar, and Kaden R. A. Hazzard. Universal thermodynamics of an $SU(n)$ fermi-hubbard model. *Phys. Rev. A*, 104:043316, Oct 2021.
- [63] Yuan Da Liao, Xiao Yan Xu, Zi Yang Meng, and Yang Qi. Gross-neveu and deconfined quantum criticalities in an extended hubbard model on the square lattice. *arXiv preprint arXiv:2204.04884*, 2022.
- [64] Xiao Yan Xu, K. T. Law, and Patrick A. Lee. Kekulé valence bond order in an extended hubbard model on the honeycomb lattice with possible applications to twisted bilayer graphene. *Phys. Rev. B*, 98:121406, Sep 2018.
- [65] Yuan-Da Liao, Xiao-Yan Xu, Zi-Yang Meng, and Jian Kang. Correlated insulating phases in the twisted bilayer graphene. *Chinese Physics B*, 30(1):017305, jan 2021.
- [66] Yuan Da Liao, Jian Kang, Clara N. Breiø, Xiao Yan Xu, Han-Qing Wu, Brian M. Andersen, Rafael M. Fernandes, and Zi Yang Meng. Correlation-induced insulating topological phases at charge neutrality in twisted bilayer graphene. *Phys. Rev. X*, 11:011014, Jan 2021.
- [67] Gaopei Pan, Xu Zhang, Heqiu Li, Kai Sun, and Zi Yang Meng. Dynamical properties of collective excitations in twisted bilayer graphene. *Phys. Rev. B*, 105:L121110, Mar 2022.
- [68] Xu Zhang, Kai Sun, Heqiu Li, Gaopei Pan, and Zi Yang Meng. Superconductivity and bosonic fluid emerging from moiré flat bands. *arXiv preprint arXiv:2111.10018*, 2021.
- [69] Charles J Geyer. Introduction to markov chain monte carlo. *Handbook of markov chain monte carlo*, 20116022:45, 2011.
- [70] Masuo Suzuki. Relationship between d-Dimensional Quantal Spin Systems and (d+1)-Dimensional Ising Systems: Equivalence, Critical Exponents and Systematic Approximants of the Partition Function and Spin Correlations. *Progress of Theoretical Physics*, 56(5):1454–1469, 11 1976.
- [71] Hans Gerd Evertz, Gideon Lana, and Mihai Marcu. Cluster algorithm for vertex models. *Phys. Rev. Lett.*, 70:875–879, Feb 1993.
- [72] NV Prokof'Ev, BV Svistunov, and IS Tupitsyn. Exact, complete, and universal continuous-time worldline monte carlo approach to the statistics of discrete quantum systems. *Journal of Experimental and Theoretical Physics*, 87(2):310–321, 1998.
- [73] J. E. Hirsch, R. L. Sugar, D. J. Scalapino, and R. Blankenbecler. Monte carlo simulations of one-dimensional fermion systems. *Phys. Rev. B*, 26:5033–5055, Nov 1982.
- [74] Anders W Sandvik and Juhani Kurkijärvi. Quantum monte carlo simulation method for spin systems. *Physical Review B*, 43(7):5950, 1991.
- [75] AW Sandvik. A generalization of handscomb's quantum monte carlo scheme-application to the 1d hubbard model. *Journal of Physics A: Mathematical and General*, 25(13):3667, 1992.
- [76] S. R. White, D. J. Scalapino, R. L. Sugar, E. Y. Loh, J. E. Gubernatis, and R. T. Scalettar. Numerical study of the two-dimensional hubbard model. *Phys. Rev. B*, 40:506–516, Jul 1989.
- [77] Xi Dai. Quantum monte carlo simulations in momentum space. *Chinese Physics Letters*, 39(5):050101, 2022.
- [78] Hans De Raedt and Ad Legendijk. Monte carlo simulation of quantum statistical lattice models. *Physics Reports*, 127(4):233–307, 1985.
- [79] Ghassan George Batrouni and Richard T. Scalettar. World-line quantum monte carlo algorithm for a one-dimensional bose model. *Phys. Rev. B*, 46:9051–9062, Oct 1992.
- [80] Hale F Trotter. On the product of semi-groups of operators. *Proceedings of the American Mathematical Society*, 10(4):545–551, 1959.
- [81] Masuo Suzuki. General correction theorems on decomposition formulae of exponential operators and extrapolation methods for quantum monte carlo simulations. *Physics Letters A*, 113(6):299–300, 1985.
- [82] RM Fye. New results on trotter-like approximations. *Physical Review B*, 33(9):6271, 1986.
- [83] RM Fye and RT Scalettar. Calculation of specific heat and susceptibilities with the use of the trotter approximation. *Physical Review B*, 36(7):3833, 1987.
- [84] NV Prokof'Ev, BV Svistunov, and IS Tupitsyn. Exact, complete, and universal continuous-time worldline monte carlo approach to the statistics of discrete quantum systems. *Journal of Experimental and Theoretical Physics*, 87(2):310–321, 1998.
- [85] F Barahona. On the computational complexity of ising spin glass models. *Journal of Physics A: Mathematical and General*, 15(10):3241–3253, oct 1982.
- [86] M. Hohenadler, Z. Y. Meng, T. C. Lang, S. Wessel, A. Muramatsu, and F. F. Assaad. Quantum phase transitions in the kane-mele-hubbard model. *Phys. Rev. B*, 85:115132, Mar 2012.
- [87] ZI YANG MENG, HSIANG-HSUAN HUNG, and THOMAS C. LANG. The characterization of topological properties in quantum monte carlo simulations of the kane–mele–hubbard model. *Modern Physics Letters B*, 28(01):1430001, 2014.
- [88] Xiao Yan Xu, Yang Qi, Long Zhang, Fakher F. Assaad, Cenke Xu, and Zi Yang Meng. Monte carlo study of lattice compact quantum electrodynamics with fermionic matter: The parent state of quantum phases. *Phys. Rev. X*, 9:021022, May 2019.
- [89] Wei Wang, Da-Chuan Lu, Xiao Yan Xu, Yi-Zhuang You, and Zi Yang Meng. Dynamics of compact quantum electrodynamics at large fermion flavor. *Phys. Rev. B*, 100:085123, Aug 2019.
- [90] Lukas Janssen, Wei Wang, Michael M. Scherer, Zi Yang Meng, and Xiao Yan Xu. Confinement transition in the qed₃-gross-neveu-xy universality class. *Phys. Rev. B*, 101:235118, Jun 2020.

- [91] Marco Cristoforetti, Francesco Di Renzo, Abhishek Mukherjee, and Luigi Scorzato. Monte carlo simulations on the lefschetz thimble: Taming the sign problem. *Physical Review D*, 88(5):051501, 2013.
- [92] Masafumi Fukuma, Nobuyuki Matsumoto, and Naoya Umeda. Applying the tempered lefschetz thimble method to the hubbard model away from half filling. *Physical Review D*, 100(11):114510, 2019.
- [93] Abhishek Mukherjee and Marco Cristoforetti. Lefschetz thimble monte carlo for many-body theories: A hubbard model study. *Physical Review B*, 90(3):035134, 2014.
- [94] Abhishek Mukherjee, Marco Cristoforetti, and Luigi Scorzato. Metropolis monte carlo integration on the lefschetz thimble: Application to a one-plaquette model. *Physical Review D*, 88(5):051502, 2013.
- [95] TC Mooney, Jacob Bringewatt, and Lucas T Brady. Lefschetz thimble quantum monte carlo for spin systems. *arXiv preprint arXiv:2110.10699*, 2021.
- [96] Petr A. Mishchenko, Yasuyuki Kato, and Yukitoshi Motome. Quantum monte carlo method on asymptotic lefschetz thimbles for quantum spin systems: An application to the kitaev model in a magnetic field. *Phys. Rev. D*, 104:074517, Oct 2021.
- [97] Michael Körner, Kurt Langfeld, Dominik Smith, and Lorenz von Smekal. Density of states approach to the hexagonal hubbard model at finite density. *Phys. Rev. D*, 102:054502, Sep 2020.
- [98] Augustin Banyaga and David Hurtubise. *Lectures on Morse homology*, volume 29. Springer Science & Business Media, 2004.
- [99] Edward Witten. A new look at the path integral of quantum mechanics. *arXiv preprint arXiv:1009.6032*, 2010.
- [100] Edward Witten. Analytic continuation of chern-simons theory. *AMS/IP Stud. Adv. Math*, 50:347, 2011.
- [101] Takuya Kanazawa and Yuya Tanizaki. Structure of lefschetz thimbles in simple fermionic systems. *Journal of High Energy Physics*, 2015(3):1–36, 2015.
- [102] R Bharathkumar and Anosh Joseph. Lefschetz thimbles and quantum phases in zero-dimensional bosonic models. *The European Physical Journal C*, 80(10):1–20, 2020.